




Energo Enviro Economic Analysis of Photovoltaic Module with Multiple Passive Thermal Management Techniques

T. K. Manoj*, U. C. Arunachala**, K. Varun*

* Renewable Energy Center, Dept. of Mech. & Ind. Engg., Manipal Institute of Technology, Manipal Academy of Higher Education, Manipal – 576104, Karnataka State, India

** Renewable Energy Center, Dept. of Mech. & Ind. Engg., Manipal Institute of Technology, Manipal Academy of Higher Education, Manipal – 576104, Karnataka State, India

(manojtk889@gmail.com, arun.chandavar@manipal.edu, varun.naik.1995@gmail.com)

‡ Corresponding Author; U. C. Arunachala, Renewable Energy Center, Dept. of Mech. & Ind. Engg., Manipal Institute of Technology, Manipal Academy of Higher Education, Manipal – 576104, Karnataka State, India, Tel: +91-820-2925461, arun.chandavar@manipal.edu

Received: 28.11.2022 Accepted:17.01.2023

Abstract- Despite the advantage of direct power generation in Photovoltaics (PV), efficiency decrement with an increased working temperature is a major challenge. Hence the present experimental study undertook three prominent passive thermal management techniques among different methods reported in the literature, and the performance was compared under identical operating conditions. Out of two PV modules, one is the reference (PV-REF), and the other is subjected to different cooling, viz. natural circulation loop (PV-NCL), burlap (PV-BUR), and front cooling (PV-FC). In PV-NCL unit, a duct at the rear surface acts as the heater, while the finned tube is the cooler. PV-BUR cooling is employed by attaching burlap fabric to the module's rear surface, where water is trickling. In the case of PV-FC, a water pipe with tiny holes is placed at the top of the PV's front surface. The experimentation shows that the temperature reduction (compared to PV-REF) in PV-NCL, PV-BUR, and PV-FC modules are 3.2°C, 11.6°C, and 24.6°C respectively, which yields a power increment of 8.2%, 16.2%, and 18.7%. On the enviro-economic front, the payback period is 2.9, 11.7, 2.7, and 2.1 years, and the corresponding values of CO₂ mitigation are 0.69, 0.73, 0.80, and 0.82 tons respectively. Thus, PV-BUR acts as a prospective competitor for PV-FC, and on the other hand, PV-NCL requires some design modifications to achieve better results.

Keywords - PV with NCL; gravity assisted flow; front cooling; enviro-economic analysis; payback period.

1. Introduction

Ever-increasing population and industrial activities forced fossil fuel usage to its peak, resulting in global warming and the fast depletion of such sources. Hence harnessing clean energy sources is the best option for mankind. Amongst many such sources, solar energy can fulfil present-day energy demands to a greater extent [1], [2]. It can be harvested in the PV route and the thermal route. Although solar thermal systems exhibit higher energy conversion efficiency [3], initial cost, a large number of components, operational difficulties etc., pave the path for PV technology, which has a feature of direct energy conversion, despite low operating efficiency [4]–[6].

When the PV module is exposed to sunshine, nearly 15-20% of irradiance is converted to electricity. Hence the remaining component results in heat accumulation, thereby causing high operating temperature and low power output. The optimum working temperature of PV cells is 25-35°C; above this, the efficiency drops by 0.45%/°C rise in temperature [7]. Eventually, very high operating temperatures damage the PV cells, causing the PV module's failure. Hence, PV module cooling is essential to enhance efficiency and improve service life. PV cooling can be achieved through optical treatment and thermal management. In optical treatment, the temperature of the PV module is restricted by radiative cooling, managing sub-bandgap absorption, and a combination of spectral and radiative cooling. However, optical treatments are not economical due to various practical

limitations. Another method of enhancing the PV module performance is the use of dye sensitized solar cells, which have been investigated in recent days [8]–[12]. On the other hand, the thermal management of PV modules is widely employed either in active or passive ways because of its numerous advantages. Although active cooling applications are dominant, the salient features of passive cooling, like power-free operation, sustainable mechanism, and low cost, followed by a sensible heat-carrying capability, made that system stand along with its counterpart. Out of various passive techniques, viz. Fins [13], PCM [14], heat pipes [15] etc., gravity-assisted water cooling and evaporative cooling are worth investigating due to their better heat-carrying capacity [16].

Gravity-assisted cooling has gained momentum in recent years. Wei He et al. [17] compared the conventional flat plate solar collector with a hybrid PV-thermal (PV/T) flat plate collector. The thermal efficiency of the PV/T collector was 40% against 75% in the traditional thermosiphon flat plate collector. On the other hand, the PV energy conversion efficiency of PV/T system was found to be 10%, which is slightly lower than that of the reference PV module. However, the primary energy savings of PV/T system was more than that of the thermosiphon collector and reference module. A similar concept termed natural circulation was used by Shi et al. [18], wherein the performance of PV/T system was analyzed under simulated solar radiation. The circulating fluid velocity (water) increased with radiation, improving thermal and overall efficiency. Further, it was found that the natural circulation phenomena exhibit hysteresis (delay in response), which makes it suitable only for small PV systems. An innovative natural circulation technique was employed by Sudhakar et al. [19], wherein the performance of a reference PV module was compared with a PV-PCM module combined with an open natural circulation system. The natural circulation of water (flow from bottom to top) was compared with the gravity-assisted flow (flow from top to bottom). The latter outperformed with an efficiency enhancement of 12.4%. Due to gravity-assisted flow's dominance, Dida et al. [20] used an interesting passive method to cool the PV module. The capillary mechanism (with burlap cloth) was amalgamated to achieve a continuous water flow. The burlap cloth was entirely in contact with the module's rear surface, and the cooling of the PV was made possible by the constant flow of water through the cloth. The temperature drop of the burlap-cooled PV module was 20°C compared to the standard PV module, which resulted in a 14.7% improvement in efficiency. Even the water consumption rate of 0.39 l/h upheld the efficacy of this technique. Further, Malvika et al. [16] compared the effect of the number of layers of burlap fabric on PV cooling. It was observed that with two layers of burlap fabric, the efficiency improved by 21% compared to the standard PV module.

In an extensive literature review by Gharzi et al. [21], various active, passive, and combined methods of cooling a solar PV module were discussed, and evaporative cooling was identified as one of the emerging passive cooling techniques. Alami [22] investigated the feasibility of using synthetic clay for evaporative cooling. The rear surface of the PV module was fitted with a perforated copper plate to which the synthetic clay layer was attached. The cooling was achieved through the

evaporation of a thin film of water over the clay, which led to a 19.1% enhancement (compared to the reference module) in power produced. Drabiniok and Neyer [23] used a bionic evaporation foil in conjunction with a PV cell. A bionic film made of two-layered dry film resist was integrated with the PV cell by laminating it over the silicon substrate. This system achieved PV cooling in a process similar to the transpiration in plants. The water evaporated through the polymer foil's micropores, leading to an 11.7°C drop in the PV cell temperature. Chandrasekar et al. [24] incorporated a cotton wick at the rear surface of the PV module and compared its performance with water and nanofluids ($\text{Al}_2\text{O}_3/\text{water}$ and CuO/water) against the reference module. A 17% drop in temperature was achieved with water against 11% in nanofluids as nanoparticles stuck to the wick, which disrupted the capillary force. Further, the fin and wick combination was attempted by Chandrasekar and Senthilkumar [25]. This technique led to a 12% drop in temperature compared to the reference module, thereby increasing the output power by 14%. Even coconut coir pith was used for evaporative cooling. Ramkiran et al. [26] used water-soaked coconut coir, which cooled the module by heat absorption and subsequent evaporation. Due to the absence of continuous water film, the temperature drop observed was only 6.2°C.

Apart from evaporative cooling and gravity-assisted rear cooling, the front surface cooling by gravity-assisted water flow is also considered a passive cooling technique. The front surface cooling technique was first investigated by Krauter [27], which reduced the surface temperature and irradiance. A thin film water flow was maintained without the use of a pump. Since the refraction index of water is less than that of glass, the temperature of the PV module was reduced by 22°C, which led to a 10.3% enhancement in the power output. In addition, the front surface cooling also aids in keeping the PV surface clean. Similarly, Smith et al. [28] proposed front cooling for PV modules used in high-temperature regions and for cooling concentrated PV systems. Moharram et al. [29] devised a strategy based on maximum allowable temperature (MAT) and combined it with the cooling of the PV panel by water spraying to optimize the amount of water utilized in the front surface cooling technique. Two cooling models were developed, viz. cooling rate model and the heating rate model. In the cooling model, the water flow was continuous, whereas in the heating model, the water flow was initiated when the module temperature crossed MAT of 45°C. The latter proved beneficial as the PV output energy exceeds the energy needed for cooling the module. Further, Odeh and Behnia [30] studied the front cooling technique and proposed it as an addition to the irrigation water supply. The system consisted of a PV module that charges a battery and runs the irrigation pump (12 V DC). Using this technique, a 15% improvement in the power output was observed. The system was simulated in TRNSYS, which depicted a 5% annual increment in energy from the PV-irrigation system. Another innovative application of the front cooling technique was studied by Arefin [31], wherein the water from an overhead tank is supplied to the PV surface, which after its cooling operation, is fed to a thermosiphon solar collector, and finally, the hot water is stored in an insulated tank. This technique led to a 1.5% increment in the PV efficiency and yielded an overall efficiency of 80%.

However, the study was numerical and lacked strong experimental confirmation.

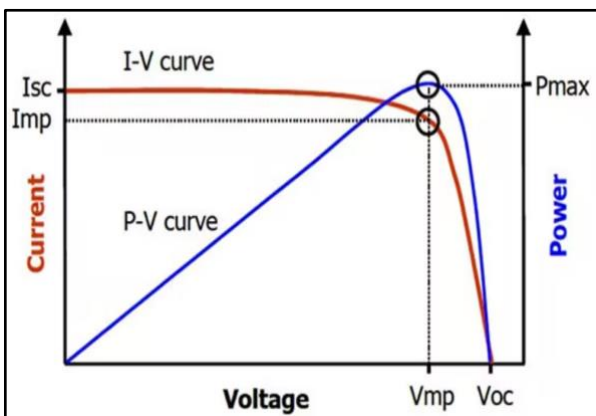
From the literature survey, it can be deduced that numerous studies have focused on the effect of fins and PCM in PV thermal management. However, these studies have limited scope due to inherent constraints. Hence recent studies have concentrated on water-based passive cooling, which includes evaporative cooling and gravity-assisted front and rear cooling. Materials like wick, burlap, and coir have been used for this purpose.

Although fin-based cooling is economical, its performance relies on the surrounding atmosphere. PCM regulates the module temperature, but the charging and discharging mode is not effective due to lower thermal conductivity. In gravity-assisted flow (with a duct attached to the rear surface), the flow rate needs to be high to compensate for the contact resistance. Further, evaporative cooling applied to the rear side results in a temperature gradient due to a differential evaporation rate. However, front cooling is very effective as it cools and cleans the module. Hence a comparative energy study is planned to evaluate the performance of the conventional front cooling technique, modified (presence of burlap cloth [20] instead of the duct [19]) gravity-assisted rear cooling, and an innovative natural circulation loop based PV cooling (PV-NCL). It is the true passive cooling technology compared to the earlier two, which are basically semi-passive technologies as water flow is once through basis from a certain elevation. This series of tests is planned indoors to have a fair comparison. Also, the environmental analysis is done to uphold the supremacy of particular passive thermal management technology. Ultimately, the best technique can be highlighted by referring to both energy and environmental analysis.

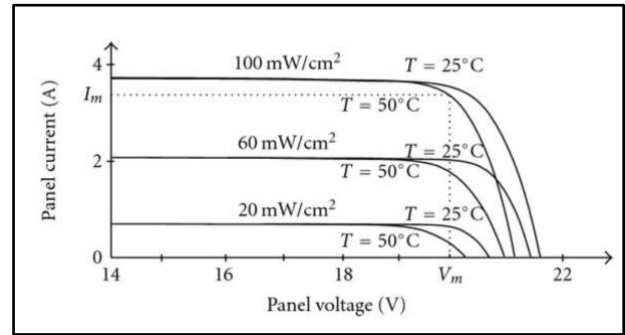
2. Analysis of PV/T System

The temperature of the PV module affects its performance and characteristics (I-V and P-V), as shown in Fig. 1 (a). The effect of temperature and irradiance on power output is depicted in Fig. 1 (b). For a specified operating load, the maximum power (P_{max}) is the product of maximum voltage (V_m) and maximum current (I_m) delivered by the module [16].

$$P_{max} = I_m * V_m \tag{1}$$



(a)



(b)

Fig. 1. (a) I-V and P-V characteristics [32]; (b) Effect of temperature on I-V characteristics [33]

PV module energy efficiency is given by [16],

$$\eta_e = \frac{P_{max}}{IA} \tag{2}$$

I is the irradiance, and module area is A.

Energy pay back time (EPBT) is the total time the system takes for energy savings to offset energy invested. It is a key factor in finalizing better energy conversion technology. In the present case, embodied energy (E_{in}) is based on different components, viz. PV module, aluminium duct, cooler, pipe fitting, piping, burlap, mesh, and wooden strip. The energy delivered by PV module is E_{out} .

$$EPBT = \frac{E_{in}}{E_{out}} \tag{3}$$

In clean energy-based power generation, eradicating harmful greenhouse emissions is quite significant compared to its counterpart, i.e. conventional energy systems. Hence CO₂ mitigation rate [34] based environmental analysis was done. Further, environmental analysis is done considering financial incentives (carbon credits) to regulate greenhouse emissions and sensitise the stake holders. Considering the CO₂ liberation rate of ≈ 2 kg/kWh [35] in fossil fuel-based power stations, the environmental parameter is defined as:

$$\phi_{CO_2} = \frac{2(E_{out} \times n)}{1000} \tag{4}$$

Where n is the lifespan of the PV module. Further, a carbon credit is given by [36]:

$$Z_{CO_2} = z_{CO_2} \times \phi_{CO_2} \tag{5}$$

Where, Z_{CO_2} is the environmental parameter and z_{CO_2} is the global carbon value (14.5 \$/ton) [37].

3. Experimental Setup and Operating Procedure

This section includes the constructional details of the experimental test rig and instrumentation for different settings.

3.1. PV Module

Two polycrystalline PV modules of the same rating (Table 1) were used here. One was the reference module (PV-REF), and the other was subjected to different thermal management techniques, i.e. natural circulation loop (NCL), burlap (BUR), fabric-based gravity-assisted flow, and front cooling (FC).

Table 1. Specification of PV module

Maximum Power (P_{max})	46.074 W
Maximum Voltage (V_{max})	19.92 V
Maximum Current (I_{max})	2.26 A
Short Circuit Current (I_{sc})	2.34 A
Open Circuit Voltage (V_{oc})	23.69 V
Maximum System Voltage	600 V
Application Class	A
Maximum Over Current Rating	4A
Country of Origin	INDIA
Manufactured Date	27-10-2020
Safety Class	11

3.2. PV-NCL unit

NCL had an aluminium duct at the bottom (heater). Finned copper cooler at the top, connected by PVC pipes (insulated) as shown in Fig. 2. The loop was then attached to the rear surface of the PV module with thermal paste and referred to as PV-NCL (Fig. 3). The entire loop was filled with water. During the operation, the hot water from the duct rose in the hot leg, reached the cooler, and returned to the duct through the cold leg. At the top, expansion tanks were provided to allow free expansion of loop fluid. To measure temperature at different sections, Pt-100 sensors were attached to the entry and exit of the duct as well as cooler, mid-portion of hot leg and cold leg. Additionally, five K-type thermocouples were pasted to the PV rear surface, as shown in Fig. 4.



Fig. 3. PV-NCL unit

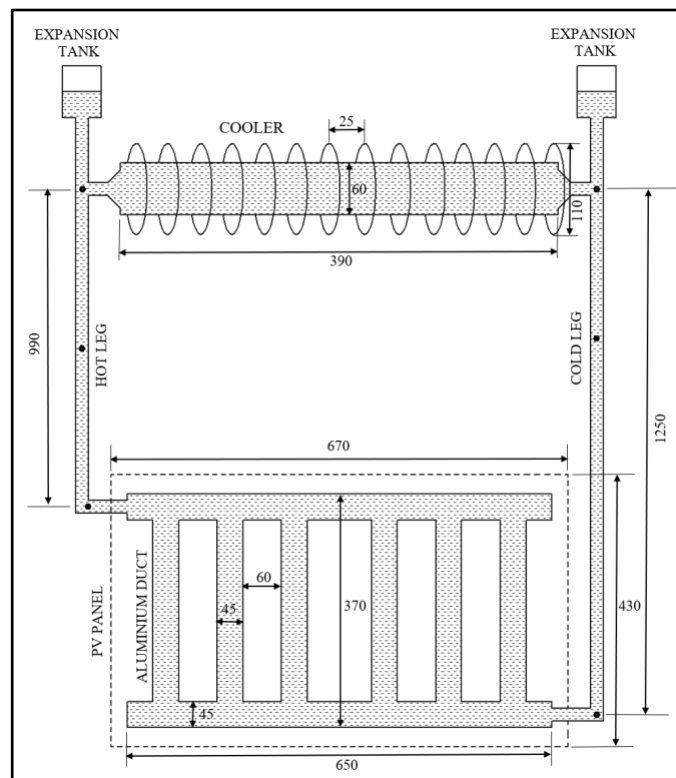


Fig. 2. Schematic of NCL

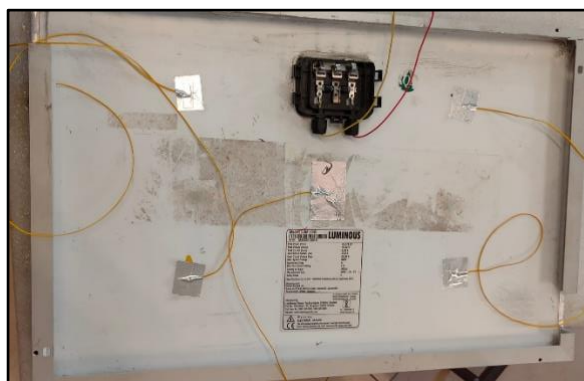


Fig. 4. Thermocouple position in PV module

3.3. PV-burlap Unit

Burlap is a flexible cloth made of vegetable fibre. In this case, the gravity-assisted flow (from the water container) was directed to the PVC pipe (with tiny holes), which was attached to the module's rear surface. Over the pipe, the burlap cloth was covered (Fig. 5) so that water could soak through the cloth (providing uniform cooling), and excess quantity could be collected at the bottom of the module. Wooden strips and steel mesh were used to hold the burlap intact with the module surface.

3.4. PV-front Cooling Unit

Here, a PVC pipe (0.5" diameter) with small holes (0.5 mm diameter) along its length was placed on the front top surface of the module, as shown in Fig. 6. The diameter and pitch of the holes were done in such a way that a thin film of

water forms over the surface. The other end of the pipe was connected to the water container through a valve. At the bottom, a provision was made to collect water. To avoid radiation effect, the pipe's outer surface was covered with reflective tape.

3.5. Experimental Setup

Figure 7 shows the schematic of the experimental setup. Every time the PV-REF was compared with the modified module, i.e. PV-NCL, PV-BUR and PV-FC. The module support structure was designed to easily fix and expose any modified module to a solar simulator. A selector switch connects both modules to a PV analyzer (MECO 9009B). All the thermocouples and Pt-100 sensors were connected to the data logger (Agilent 34972A). A laptop was connected to a PV analyzer and data logger to store real-time data. The desired radiation level was managed with the help of halogen lamps based solar simulator (3000 W) and a digital sunshine recorder (Kaizen Imperial). The room temperature variation was 32°C to 34°C during the test period.



Fig. 5. Rear surface of PV module covered with burlap



Fig. 6. PV front cooling arrangement

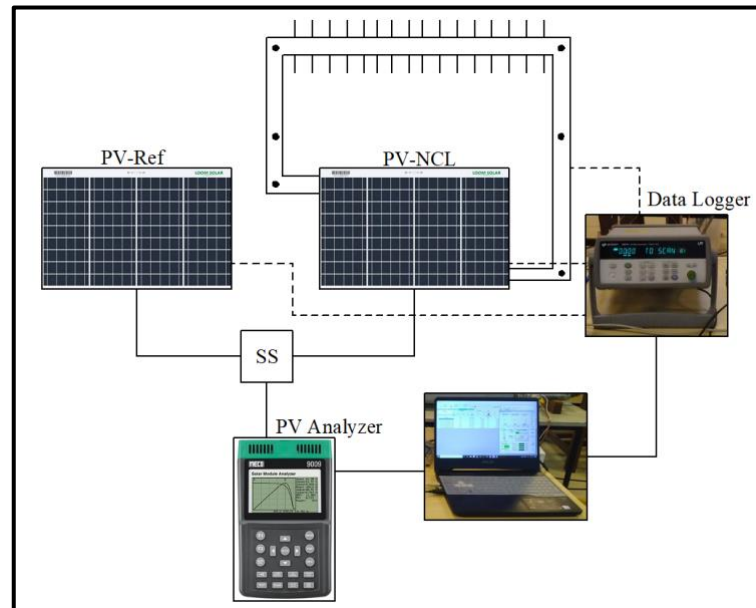


Fig. 7. Schematic of the experimental set up

3.6. Operating Procedure

The experimental procedure to test both reference and modified modules is detailed below.

1. Initially, the reference PV module was positioned perpendicular to the light rays of the solar simulator (inclined at 45°).
2. The radiation level was set to 300 W/m² with a digital sunshine recorder, and the data logger was switched ON and set to a scan time of 10 s. Once the irradiance and module temperatures (five points) were stabilized (≈20 minutes), the PV analyzer recorded energy parameters (V_{max}, I_{max}, P_{max}) and PV characteristics.
3. The same procedure was followed in case of other irradiance i.e. 400, 500 and 600 W/m².
4. Later, one of the modified modules (say PV-NCL) replaced the PV-REF, and the earlier procedure was continued. Here, the temperature points were more, i.e. six locations in the NCL and five points over the module's rear surface.
5. In the case of PV-BUR, the flow rate from the water container to the module was regulated by the valve, and the value set was 0.16 lpm (optimized) for the irradiance range.
6. Similarly, flow rates of 0.16 lpm and 0.25 lpm were attempted for PV-FC to study the cooling effect.

Prior to the testing, pre-requisites are;

- PV-NCL: The loop must be filled with water at room temperature till half of the expansion tank.
- PV-BUR: The burlap cloth should be wet by spraying water over it.

4. Results and Discussion

This section includes the PV-REF module’s performance comparison (both energy and enviro-economic) with the PV-NCL, PV-BUR and PV-FC techniques.

4.1. PV Thermal Management

It includes module temperature variation, power output, electrical efficiency, and P-V characteristics.

(a) Module temperature

PV-FC mechanism has its own advantage and disadvantages, the benefit being the removal of dust during cooling of the module, while the irradiance drops due to the masking of water film over the surface. Hence, flow optimization is a crucial task. Accordingly, the flow rate of 0.16 lpm and 0.25 lpm were used and termed as front cooling low (FCL) and front cooling high (FCH). In the case of FCL, the maximum temperature drop observed is 50% against 62% for FCH compared to PV-REF (Fig. 8). It is worth noting that, although the flow rate is $\approx 50\%$ more, the difference in temperature drop between FCH and FCL is merely 2 to 9%. The higher heat-carrying capacity of water and reduced irradiance due to the thick water film over the surface are the reason for it. Henceforth, only the FCL case is considered for comparison with other modules.

Figure 9 shows the module temperature variation with irradiance for all cases. PV-FCL results in the best temperature drop, followed by PV-BUR, and the least improvement is observed in case of PV-NCL. For example, at 600 W/m^2 , the temperature reduction in PV-NCL, PV-BUR, and PV-FCL is 3.2°C (4.5%), 11.6°C (18.8%), and 24.6°C (50.5%) respectively compared to PV-REF. Similarly, at 300 W/m^2 these observations are 3.3°C (5.8%), 9.6°C (19%), and 19.1°C (46.6%). Except for PV-NCL, in the rest the cases (including PV-REF), the module temperature is taken as the average of five points (refer Fig. 10). However, only the temperature at the midpoint is taken for PV-NCL, which was not covered by duct. This is justified as $\approx 50\%$ of the rear surface area was not covered by the duct.

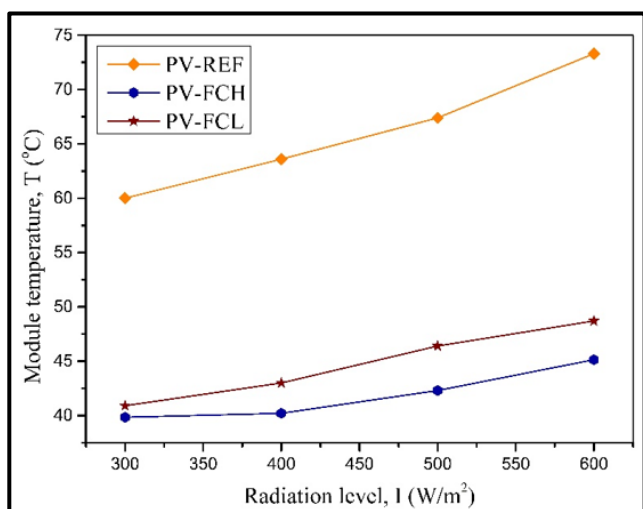


Fig. 8. Module temperature with front cooling

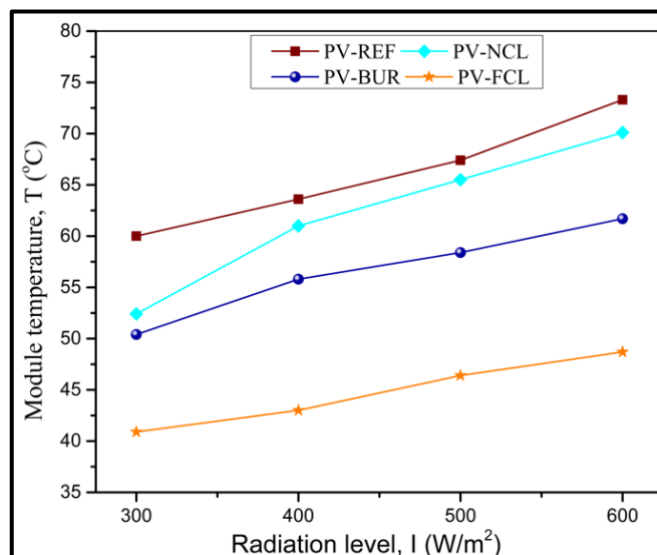


Fig. 9. Module temperature variation with different types of passive cooling

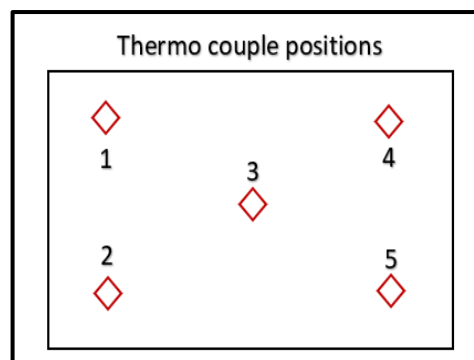


Fig. 10. Thermocouples position

Further, the temperature distribution along the PV module rear surface in all cases is shown in Fig. 11. An interesting observation is that except PV-NCL, in rest all cases, the temperature difference between the midpoint (T_3) and left side (T_1, T_2) or right side (T_4, T_5) of the module is not significant. Since the heat accumulation is more at the centre, the temperature (T_3) is high in every case. However, in PV-NCL, a peculiar behavior is seen as the module centre temperature is very high. As mentioned earlier, the region of T_3 was not covered by the duct, while the other four points (T_1, T_2, T_4, T_5) were sandwiched between the module and the duct. Further, a notable difference in power output is expected as $\approx 50\%$ of the module is covered by the duct.

Hence, as far as thermal management of the PV module is concerned, front cooling mechanism is the best. However, owing to the energy consumed for cooling the PV module, NCL technique (with certain modifications) is viable due to its passive nature.

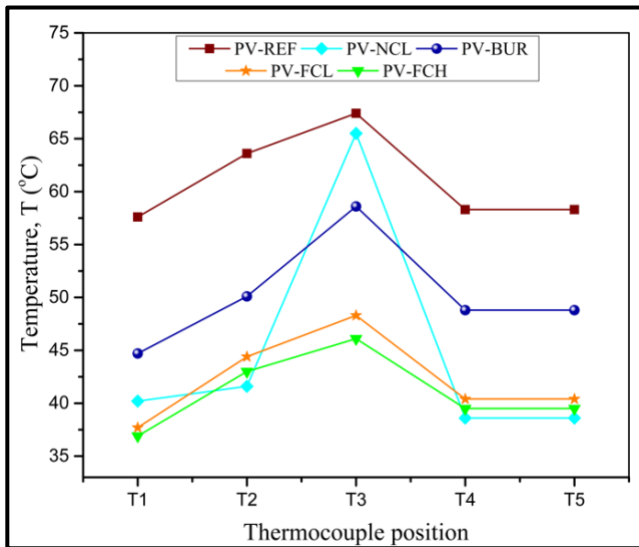


Fig. 11. Temperature gradient within the module

(b) Flow phenomena in NCL

As mentioned earlier, in simple NCL, the heater is located at the bottom, and the cooler is at the top, which are connected by two pipes (hot leg and cold leg) to complete the loop. The heater and condenser are connected by two pipes representing the natural circulation loop. As seen in Fig. 2, the left leg is connected to the top end of the module, whereas the right leg is from the bottom. Hence during heating, due to buoyancy force, the water comes out of the heater (duct), enters the left leg, and reaches the cooler. Subsequently, the water discharged from the cooler enters the bottom end of the heater through the right vertical leg. Hence there is a natural circulation of coolant within the loop due to the temperature difference between the heater and the cooler.

Figure 12 shows the temperature of the coolant (water) at different locations in the NCL. The temperature sensors were positioned at the heater entry (H_{in}), heater exit (H_{out}), hot leg (H_{leg}), condenser entry (C_{in}), cooler exit (C_{out}), and cold leg (C_{leg}). This kind of sensor arrangement facilitates loop fluid flow direction. For example, in case of 400 W/m^2 , water entered the PV module at 34.2°C , and after extraction of heat, came out at 37.3°C . In the hot leg, the temperature dropped to 36.2°C . Later it entered the cooler at 36.1°C , and after heat dissipation, the fluid exit temperature was 34.5°C . Finally, the cooled fluid entered the heater through the cold leg, where it was at 32.8°C . It is worth noting that the coolant temperature at the heater entry is more than the cold leg temperature. This is because of the accumulation of a small amount of hot water at the heater entry (hot pocket). A temperature drop was noticed in both hot and cold legs due to heat loss to the surrounding.

(c) Power output

The cooling effect directly influences the power output. Figure 13 compares the power output of PV-REF with the other three passive methods. At 300 W/m^2 , the power produced by PV-NCL, PV-BUR, PV-FCL are 5.8%, 14.6%, and 14.4% more than that of PV-REF. Similarly, at 600 W/m^2 the increment is 6.5%, 16.17%, and 18.6% respectively. It has

been observed that till 400 W/m^2 both PV-BUR and PV-FCL are performing equally and thereafter, PV-FCL dominates by a small margin. This justifies the efficacy of PV-FCL over PV-BUR. Although the same flow rate has been maintained in both cases, the exposure of water film directly to the ambient in PV-FCL results in better cooling. However, in PV-BUR, the burlap layer acts as a barrier for water from losing heat with the surrounding.

(d) Electrical efficiency

Although the energy conversion efficiency improved with cooling, the general trend of drop in efficiency with increment in irradiance is observed due to elevated operating temperature. In Fig. 14, till 400 W/m^2 , both PV-BUR and PV-FCL perform equally, as the corresponding efficiency is 8.51% and 8.53% respectively. Thereafter PV-FCL dominates by a small margin of $\approx 2\%$. Apart from the best performance of PV-FCL, in practical application also, this method is preferred as it can remove the dust accumulated over the top surface. On the other hand, such an additional advantage is not possible with PV-BUR.

Although PV-NCL outperforms PV-REF, the performance enhancement is minimal compared to PV-BUR and PV-FCL. This is because the duct used in the present study had less area of contact ($\approx 50\%$) with the module's rear surface. As an outcome, the temperature across the surface was non-uniform. However, this limitation can be overcome by forming a duct so that water can directly come in contact with the rear surface.

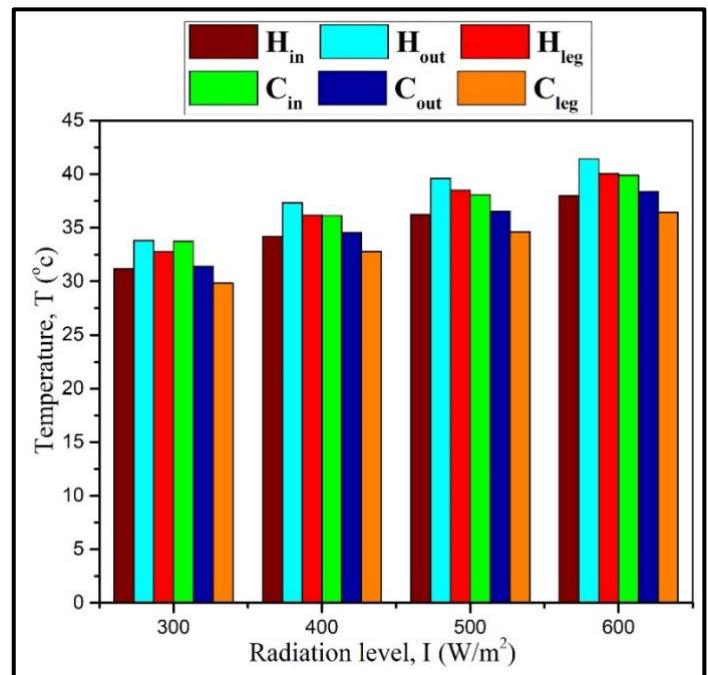


Fig. 12. Coolant temperature at different locations in NCL

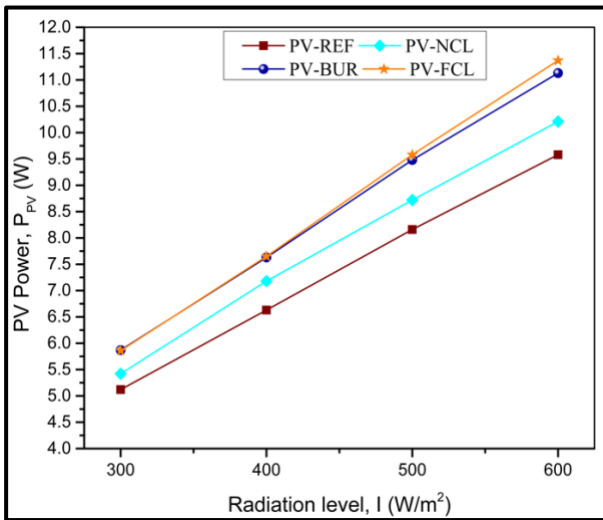


Fig. 13. Power output in different modules

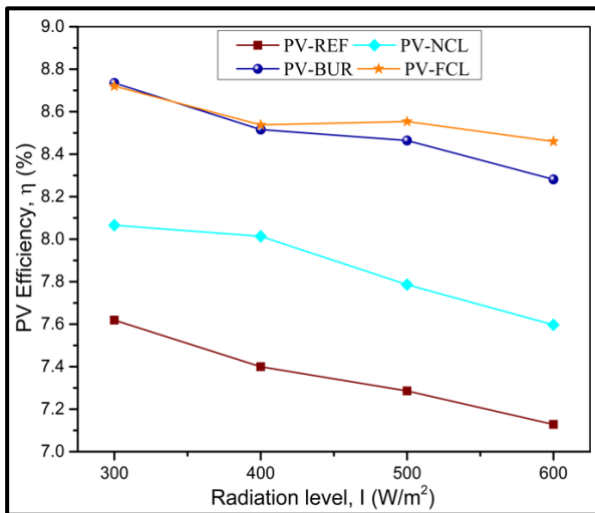


Fig. 14. Efficiency variation with irradiance

4.2. Enviro-economic Analysis

It includes the energy payback period, economic payback period, and carbon mitigation rate.

(a) Energy payback period

The embodied energy content in different PV models is listed in Table 2. The conventional unit (PV-REF) has the least value, whereas the PV-NCL denotes the maximum as multiple materials are involved. The embodied energy increment of 77%, 9%, and 2.2% (compared to PV-REF) for PV-NCL, PV-BUR, and PV-FCL, respectively. The PV-BUR has relatively low embodied energy due to the usage of nature-friendly items i.e., wooden strip and burlap fabric. Further, the energy payback period is calculated as listed in Table 3. Except for PV-NCL, the energy output is notable against the rise in embodied energy. To elaborate, the payback period is 21.80 years, 12.36 years, and 11.25 years for PV-NCL, PV-BUR and PV-FCL respectively, against 13.08 years for PV-REF. Here the annual energy output is calculated by considering the radiation level of 600W/m², six hours of daily operation, and 300 solar days in a year.

(b) Economic payback period

A simple economic analysis is also undertaken considering the cost of different models, as listed in Table 4. The experiments conducted depict the average electrical power generated per hour by PV-REF, PV-NCL, PV-BUR, and PV-FCL as 9.58 W, 10.21 W, 11.13 W, and 11.37 W respectively. Considering six hours of operation per day and 300 solar days (Manipal, India), the annual electrical energy output is 17.24 kWh, 18.37 kWh, 20.03 kWh, and 20.46 kWh. In continuation, the cost of 1 kWh energy generated by PV is calculated by dividing the annual electrical power generation by the total cost incurred for the system. In the case of PV-REF, the total cost incurred is only the cost of the PV module and its mounting structure. Whereas for the modified modules, additional components are considered. Further, assuming replacements of burlap cloth once in three months leads to the addition of maintenance/replacement cost. Thus, the cost of PV power generation for different modules are Rs. 150.8/kWh, Rs. 645/kWh, 160.25/kWh, and Rs. 130.98/kWh respectively. Suppose these PV modules are exclusively meant for power generation and selling to the grid without any consumption. In that case, the revenue generated can be evaluated by multiplying the annual power generated with the local tariff for PV power. In the present locality, the electricity board purchases PV power at Rs. 3/kWh. Hence the total revenue generated by these modules are Rs. 51.72, Rs. 55.11, Rs. 60.09, and Rs. 61.38 respectively. Finally, the payback period is calculated by dividing the total cost by total revenue, which yields 2.91, 11.70, 2.66, and 2.13 years respectively.

(c) Carbon mitigation

Besides energy savings, PV thermal management helps eradicate CO₂ emissions and thereby gaining carbon credit. Table 6 presents the CO₂ evasion rates for different models. The quantity of CO₂ circumvented by PV-REF, PV-NCL, PV-BUR, and PV-FCL is 0.689, 0.734, 0.801, and 0.818 tons, respectively, over the lifespan based on the energy approach. Ultimately the PV-FCL model evolved as the best based on the CO₂ evasion rate.

5. Conclusion and Future Scope

The outcome of the detailed experimental investigation is listed below:

- i. The temperature reduction (compared to PV-REF) in PV-NCL, PV-BUR, and PV-FC models is 3.2°C, 11.6°C, and 24.6°C respectively, which leads to an increment in power output of 8.2%, 16.2%, and 18.7%.
- ii. As far as the electrical efficiency enhancement is concerned, it follows the trend of PV-FC>PV-BUR>PV-NCL.
- iii. By looking at the temperature at different locations in the PV-NCL system, the unidirectional flow of water within the loop is confirmed.
- iv. In case of front cooling, the lower flow rate (0.16 lpm) of water resulted in higher efficiency despite better cooling witnessed with a high flow rate (0.25 lpm). The reason is a significant drop in irradiance due to the thick water film over the module.

v. Embodied energy analysis upheld the supremacy of PV-BUR and PV-FC over PV-NCL, as the energy payback time of these were 12.36, 11.25, and 21.80 years respectively, against 13.08 years for PV-REF.

vi. An economic analysis also supported the above result, as the payback periods of PV-REF, PV-NCL, PV-BUR, and PV-FC are 2.91, 11.7, 2.66, and 2.13 years respectively.

vii. The enviro-economic analysis reflected CO₂ evasion rates as 0.69, 0.73, 0.8, and 0.82 tons respectively, for PV-REF, PV-NCL, PV-BUR, and PV-FC.

The extensive analysis of different passive cooling methods also stated the scope for future work as listed below:

i. In comparison, the PV-NCL technique could not perform well due design limitation of the duct. Hence, a better design is suggested to attain uniform and efficient cooling.

ii. Although fare comparison was possible with indoor testing, the realistic behavior of PV modules with different cooling mechanisms is possible only with outdoor testing.

iii. A proper water flow mechanism must be devised in front cooling to maintain a liquid film of uniform thickness over the module area.

iv. For rear-side passive cooling, suitable porous media can also be thought of.

Table 2. Embodied energy level for PV models

Component	Quantity	Energy density	Embodied energy (kWh)			
			PV-REF	PV-NCL	PV-BUR	PV-FCL
PV module	0.226 m ²	997 kWh/m ² [38]	225.54	225.54	225.54	225.54
Flow duct (Aluminium)	1.6 kg	201MJ/kg [39]	-	89.3	-	-
Cooler (copper)	2.75 kg	70.6 MJ/kg [39]	-	52.9	-	-
Piping and fittings (PVC)	1.69 kg (NCL)	70 MJ/kg [39]	-	32.8	4.66	4.66
	0.24 kg (BUR)					
	0.24 kg (FCL)					
Burlap	400 gm	2.6 kWh/kg [40]	-	-	1.07	-
Steel mesh	250 gm	60 MJ/kg [41]	-	-	14.9	-
Wooden strip	500 gm	10.4 MJ/kg [41]	-	-	1.44	-
Total embodied energy (En_{in})			225.54	400.54	247.60	230.20

Table 3. Different PV models with energy payback time

Term	PV-REF	PV-NCL	PV-BUR	PV-FCL
En _{out} (kWh)	17.24	18.37	20.03	20.46
En _{in} (kWh)	225.54	400.54	247.60	230.2
EPBT_{en} (years)	13.08	21.80	12.36	11.25

Table 4. Total cost for different models

Items	Cost (In Indian Rupees)			
	PV-REF	PV-NCL	PV-BUR	PV-FCL
40W PV module	2600	2600	2600	2600
Duct	-	2700	-	-
Cooler	-	5150	-	-
Pipe and fittings	-	550	80	80
Thermal paste	-	850	-	-
Burlap	-	-	50 x 4	-
Steel mesh	-	-	300	-
Wooden strips	-	-	30	-
Total cost (Rs)	2600	11850	3210	2680

Table 5. Economic payback period for different models

Particulars	PV-REF	PV-NCL	PV-BUR	PV-FCL
Power generated (W)	9.58	10.21	11.13	11.37
Annual electrical energy (kWh)	17.24	18.37	20.03	20.46
Cost of the setup (Rs)	2600	11850	3210	2680
Cost of PV power generation (Rs/kWh)	150.8	645	160.25	130.98
Total Revenue generated (Savings in Rs.)	51.72	55.11	60.09	61.38
Payback period	2.91	11.70	2.66	2.13

Table 6. Enviro-economic parameters for different models

Parameter	PV-REF	PV-NCL	PV-BUR	PV-FCL
Lifespan	20	20	20	20
En _{out} –annual (kWh)	17.24	18.37	20.03	20.46
Environmental parameter (Rate ton CO ₂)	0.689	0.734	0.801	0.818
Enviroeconomic parameter (Rate \$)	10.05	10.70	11.68	11.93

References

[1] A. G. Alkholidi and H. HAMAM, “Solar Energy Potentials in Southeastern European Countries: A Case Study,” *International Journal of Smart grid*, vol. 3, no. 2, pp. 108–119, 2019, doi: 10.20508/ijsmartgrid.v3i2.51.g55.

[2] A. Harrouz, A. Temmam, and M. Abbes, “Renewable Energy in Algeria and Energy Management Systems,” *International Journal of Smart grid*, vol. 2, no. 1, pp. 34–39, 2017, doi: 10.20508/ijsmartgrid.v2i1.10.g9.

[3] K. KASSMI *et al.*, “Innovative Solar Pressure Cooker with Parabolic Trough Concentrator using Water Vapor InnovSoPre,” *International Journal of Renewable Energy Research*, vol. 12, no. 3, pp. 1216–1224, 2022, doi: 10.20508/ijrer.v12i3.13089.g8506.

[4] M. Banja and M. Jégard, “An Analysis of Capacity Market Mechanism for Solar Photovoltaics in France,” *International Journal of Smart grid*, vol. 3, no. 1, pp. 10–18, 2019, doi: 10.20508/ijsmartgrid.v3i1.36.g41.

[5] D. Siswantoro and S. L. Z. Ridho, “Is Grid Solar Power Still Attractive Amid Decreasing Fuel Prices? The Case of Indonesian Electrical Power,” *International Journal of Smart grid*, vol. 5, no. 2, pp. 83–87, Jun. 2021, doi: 10.20508/ijsmartgrid.v5i2.188.g148.

[6] F. Javed, “Impact of Temperature & Illumination for Improvement in Photovoltaic System Efficiency,” *International Journal of Smart grid*, vol. 6, no. 1, pp. 19–29, 2022, doi: 10.20508/ijsmartgrid.v6i1.222.g234.

[7] D. M. C. Shastry and U. C. Arunachala, “Thermal management of photovoltaic module with metal matrix embedded PCM,” *J Energy Storage*, vol. 28, p. 101312, Apr. 2020, doi: 10.1016/j.est.2020.101312.

[8] S. A. Taya, T. M. El-Agez, M. S. Abdel-Latif, H. S. El-Ghamri, A. Y. Batniji, and I. R. El-Sheikh, “Fabrication of dye-sensitized solar cells using dried plant leaves,” *International Journal of Renewable Energy Research*, vol. 4, no. 2, pp. 384–388, 2014, doi: 10.20508/ijrer.v4i2.1202.g6290.

[9] M. S. Abdel-Latif, T. M. Abuiriban, Mahmoud BEL-Agez, and S. A. Taya, “Dye-Sensitized Solar Cells Using Dyes Extracted from Flowers, Leaves, Parks, and Roots of Three Trees,” *International Journal of Renewable Energy Research*, vol. 5, no. 1, pp. 294–298, 2015, doi: 10.20508/ijrer.v5i1.2000.g6497.

[10] A. Batniji, M. S. Abdel-Latif, T. M. El-Agez, S. A. Taya, and H. Ghamri, “Dyes extracted from Trigonella seeds as photosensitizers for dye-sensitized solar cells,” *Journal of Theoretical and Applied Physics*, vol. 10, no. 4, pp. 265–270, Dec. 2016, doi: 10.1007/s40094-016-0225-9.

[11] S. A. Taya, T. M. El-Agez, M. S. Abdel-Latif, H. Ghamri, A. Batniji, and W. A. Tabaza, “Dyes Extracted from Safflower, Medicago Sativa, and Ros Marinius Officinalis as Photosensitizers for Dye-sensitized Solar Cells,” *Journal of Nano- and Electronic Physics*, vol. 8, no. 1, pp. 01026-1-01026–5, 2016, doi: 10.21272/jnep.8(1).01026.

[12] A. Y. Batniji, R. Morjan, M. S. Abdel-Latif, T. M. El-Agez, S. A. Taya, and H. S. El-Ghamri, “Aldimine derivatives as photosensitizers for dye-sensitized solar cells,” *TURKISH JOURNAL OF PHYSICS*, vol. 38, pp. 86–90, 2014, doi: 10.3906/fiz-1309-4.

- [13] J. Li *et al.*, "Performance evaluation of bifacial PV modules using high thermal conductivity fins," *Solar Energy*, vol. 245, pp. 108–119, Oct. 2022, doi: 10.1016/j.solener.2022.09.017.
- [14] Y. Cui, J. Zhu, F. Zhang, Y. Shao, and Y. Xue, "Current status and future development of hybrid PV/T system with PCM module: 4E (energy, exergy, economic and environmental) assessments," *Renewable and Sustainable Energy Reviews*, vol. 158, p. 112147, Apr. 2022, doi: 10.1016/j.rser.2022.112147.
- [15] W. Yao, X. Kong, X. Han, Y. Wang, J. Cao, and W. Gao, "Research on the efficiency evaluation of heat pipe PV/T systems and its applicability in different regions of China," *Energy Convers Manag*, vol. 269, p. 116136, Oct. 2022, doi: 10.1016/j.enconman.2022.116136.
- [16] A. Malvika, U. C. Arunachala, and K. Varun, "Sustainable passive cooling strategy for photovoltaic module using burlap fabric-gravity assisted flow: A comparative Energy, exergy, economic, and enviroeconomic analysis," *Appl Energy*, vol. 326, p. 120036, Nov. 2022, doi: 10.1016/j.apenergy.2022.120036.
- [17] W. He, Y. Zhang, and J. Ji, "Comparative experiment study on photovoltaic and thermal solar system under natural circulation of water," *Appl Therm Eng*, vol. 31, no. 16, pp. 3369–3376, Nov. 2011, doi: 10.1016/j.applthermaleng.2011.06.021.
- [18] Q. Shi, J. Lv, C. Guo, and B. Zheng, "Experimental and simulation analysis of a PV/T system under the pattern of natural circulation," *Appl Therm Eng*, vol. 121, pp. 828–837, Jul. 2017, doi: 10.1016/j.applthermaleng.2017.04.140.
- [19] P. Sudhakar, R. Santosh, B. Asthalakshmi, G. Kumaresan, and R. Velraj, "Performance augmentation of solar photovoltaic panel through PCM integrated natural water circulation cooling technique," *Renew Energy*, vol. 172, pp. 1433–1448, Jul. 2021, doi: 10.1016/j.renene.2020.11.138.
- [20] M. Dida, S. Boughali, D. Bechki, and H. Bouguettaia, "Experimental investigation of a passive cooling system for photovoltaic modules efficiency improvement in hot and arid regions," *Energy Convers Manag*, vol. 243, p. 114328, Sep. 2021, doi: 10.1016/j.enconman.2021.114328.
- [21] M. Gharzi, A. Arabhosseini, Z. Gholami, and M. H. Rahmati, "Progressive cooling technologies of photovoltaic and concentrated photovoltaic modules: A review of fundamentals, thermal aspects, nanotechnology utilization and enhancing performance," *Solar Energy*, vol. 211, pp. 117–146, Nov. 2020, doi: 10.1016/j.solener.2020.09.048.
- [22] A. H. Alami, "Effects of evaporative cooling on efficiency of photovoltaic modules," *Energy Convers Manag*, vol. 77, pp. 668–679, Jan. 2014, doi: 10.1016/j.enconman.2013.10.019.
- [23] E. Drabiniok and A. Neyer, "Bionic micro porous evaporation foil for photovoltaic cell cooling," *Microelectron Eng*, vol. 119, pp. 65–69, May 2014, doi: 10.1016/j.mee.2014.02.013.
- [24] M. Chandrasekar, S. Suresh, T. Senthilkumar, and M. Ganesh karthikeyan, "Passive cooling of standalone flat PV module with cotton wick structures," *Energy Convers Manag*, vol. 71, pp. 43–50, Jul. 2013, doi: 10.1016/j.enconman.2013.03.012.
- [25] M. Chandrasekar and T. Senthilkumar, "Experimental demonstration of enhanced solar energy utilization in flat PV (photovoltaic) modules cooled by heat spreaders in conjunction with cotton wick structures," *Energy*, vol. 90, pp. 1401–1410, Oct. 2015, doi: 10.1016/j.energy.2015.06.074.
- [26] R. B. S. CK, and K. Sudhakar, "Sustainable passive cooling strategy for PV module: A comparative analysis," *Case Studies in Thermal Engineering*, vol. 27, p. 101317, Oct. 2021, doi: 10.1016/j.csite.2021.101317.
- [27] S. Krauter, "Increased electrical yield via water flow over the front of photovoltaic panels," *Solar Energy Materials and Solar Cells*, vol. 82, no. 1–2, pp. 131–137, May 2004, doi: 10.1016/j.solmat.2004.01.011.
- [28] M. K. Smith *et al.*, "Water Cooling Method to Improve the Performance of Field-Mounted, Insulated, and Concentrating Photovoltaic Modules," *J Sol Energy Eng*, vol. 136, no. 3, Aug. 2014, doi: 10.1115/1.4026466.
- [29] K. A. Moharram, M. S. Abd-Elhady, H. A. Kandil, and H. El-Sherif, "Enhancing the performance of photovoltaic panels by water cooling," *Ain Shams Engineering Journal*, vol. 4, no. 4, pp. 869–877, Dec. 2013, doi: 10.1016/j.asej.2013.03.005.
- [30] S. Odeh and M. Behnia, "Improving Photovoltaic Module Efficiency Using Water Cooling," *Heat Transfer Engineering*, vol. 30, no. 6, pp. 499–505, May 2009, doi: 10.1080/01457630802529214.
- [31] Md. A. Arefin, "Analysis of an Integrated Photovoltaic Thermal System by Top Surface Natural Circulation of Water," *Front Energy Res*, vol. 7, Sep. 2019, doi: 10.3389/fenrg.2019.00097.
- [32] Sam Davis, "Solar System Efficiency: Maximum Power Point Tracking is Key." <https://www.electronicdesign.com/>
- [33] E. Durán, J. M. Andújar, J. M. Enrique, and J. M. Pérez-Oria, "Determination of PV Generator I-V/P-V Characteristic Curves Using a DC-DC Converter Controlled by a Virtual Instrument," *International Journal of Photoenergy*, vol. 2012, pp. 1–13, 2012, doi: 10.1155/2012/843185.
- [34] M. S. Yousef and H. Hassan, "An experimental work on the performance of single slope solar still

- incorporated with latent heat storage system in hot climate conditions,” *J Clean Prod*, vol. 209, pp. 1396–1410, Feb. 2019, doi: 10.1016/j.jclepro.2018.11.120.
- [35] E. Deniz and S. Çınar, “Energy, exergy, economic and environmental (4E) analysis of a solar desalination system with humidification-dehumidification,” *Energy Convers Manag*, vol. 126, pp. 12–19, Oct. 2016, doi: 10.1016/j.enconman.2016.07.064.
- [36] M. S. Yousef, H. Hassan, and H. Sekiguchi, “Energy, exergy, economic and enviroeconomic (4E) analyses of solar distillation system using different absorbing materials,” *Appl Therm Eng*, vol. 150, pp. 30–41, Mar. 2019, doi: 10.1016/j.applthermaleng.2019.01.005.
- [37] H. Hassan, M. S. Yousef, M. Fathy, and M. S. Ahmed, “Impact of condenser heat transfer on energy and exergy performance of active single slope solar still under hot climate conditions,” *Solar Energy*, vol. 204, pp. 79–89, Jul. 2020, doi: 10.1016/j.solener.2020.04.026.
- [38] M. S. Yousef, M. Sharaf, and A. S. Huzayyin, “Energy, exergy, economic, and enviroeconomic assessment of a photovoltaic module incorporated with a paraffin-metal foam composite: An experimental study,” *Energy*, vol. 238, p. 121807, Jan. 2022, doi: 10.1016/j.energy.2021.121807.
- [39] “Embodied energy coefficients.” <https://www.wgtn.ac.nz/architecture/centres/cbpr/resources/pdfs/ee-coefficients.pdf>
- [40] “Embodied energy needed to make one sofa.” <https://oecotextiles.blog/2010/01/06/embodied-energy-needed-to-make-one-sofa/>
- [41] “Embodied energy”, doi: <https://www.yourhome.gov.au/materials/embodied-energy>.